

## Initiation and Propagation of Coronal Mass Ejections

P. F. Chen

*Department of Astronomy, Nanjing University, Nanjing 210 093, China.*

*e-mail: chenpf@nju.edu.cn*

**Abstract.** This paper reviews recent progress in the research on the initiation and propagation of CMEs. In the initiation part, several trigger mechanisms are discussed; in the propagation part, the observations and modelings of EIT waves/dimmings, as the EUV counterparts of CMEs, are described.

*Key words.* Coronal mass ejections—magnetic field.

### 1. Introduction

Coronal mass ejections (CMEs) have been observed for over 30 years. They keep being an intriguing research topic, not only because they are now realized to be the major driver for space weather disturbances, which are intimately connected to human activities, but also because they themselves are full of questions that have been provoking scientists to seek for answers. Stimulated by the limited observations, theoretical researches are involved in the various phases of the eruptions from their birth to their pilgrimage in the interplanetary (IP) space. First, we are still not quite sure what is the progenitor of a CME. The rough picture is described as follows: magnetic field, which is generated at the tachocline layer, emerges throughout the convection zone and the lower atmosphere into the tenuous corona. The coronal field keeps adjusting to a more and more complex magnetic structure in a quasi-steady way. After a threshold, the magnetic structure cannot sustain its equilibrium and begins to erupt. In this picture, it is still an open question whether the pre-CME structure should always possess a flux rope. Or, the so-called flux rope is actually an extreme case of the ordinary magnetic arcade with a strong twist. The second issue is how the progenitor is triggered to deviate from the equilibrium state. In this aspect, the statistical investigations of the correlation between CME onsets and other phenomena are of extreme significance. The third issue is how a CME is accelerated. The related questions involve (1) whether magnetic reconnection is a necessary condition, (2) how important the interaction between the ejecta and the solar wind is, (3) the effect of prominence mass drainage, among others. The fourth issue is how the CME is related to the accompanied phenomena, such as solar flares, Moreton waves, EIT waves and dimmings, transient coronal holes, etc. The fifth issue is how the CME evolves to an interplanetary CME (ICME) and how the CME properties affect the geomagnetic activity.

In this review paper, we focus on two aspects of the theoretical researches on CMEs, i.e., the initiation and propagation, which are presented in sections 2 and 3, respectively. We refer the readers to Forbes (2000), Gopalswamy (2003), and Volume 123 of *Space*

*Sci. Rev.* for more detailed reviews. The chances and challenges of solar cycle 24 are briefly prospected in section 4.

## 2. Initiation of CMEs

Except some narrow CMEs, which may correspond to a jet (say, reconnection jet) propagating along open field lines, most CMEs are regarded as an erupting flux rope system, with a typical three-component structure in the white-light coronagraph images, although sometimes one or two components are absent possibly due to observational effect or the plasma has not yet condensed to form a filament at the magnetic dips of the flux rope. The eruption process can generally be described in the classical CSHKP framework: a flux rope, which may or may not host a filament, becomes unstable or loses its equilibrium, it then rises and pulls up the closed field lines straddling over it, so as to form a current sheet beneath the flux rope. The reconnection at the current sheet removes the constraint of the line-tied field lines, and the flux rope is pushed to erupt by the upward reconnection jet. Therefore, one important and unclear issue in this picture is how the flux system is triggered.

### 2.1 Emerging flux trigger mechanism

Early in the 1970s, it was found that weak X-ray activities often precede solar flares (Datlowe *et al.* 1974), which were described as the soft X-ray precursor of CMEs by Harrison *et al.* (1985). In an apparently unrelated research, Feynman & Martin (1995) found that many CMEs are strongly associated with emerging flux that possesses polarity orientation favorable for magnetic reconnection between the emerging flux and the pre-existing coronal field either inside or outside the filament channel. Wang & Sheeley (1999) confirmed the strong correlation between CMEs and reconnection-favorable emerging flux, although it is noted that not all CMEs are related to emerging flux. Motivated by such a correlation, we proposed an emerging flux trigger mechanism for CMEs (Chen & Shibata 2000), as illustrated by Fig. 1. When the reconnection-favorable emerging flux appears inside the filament channel, it cancels the small magnetic loops near the polarity inversion line (PIL). Thereby, the magnetic pressure

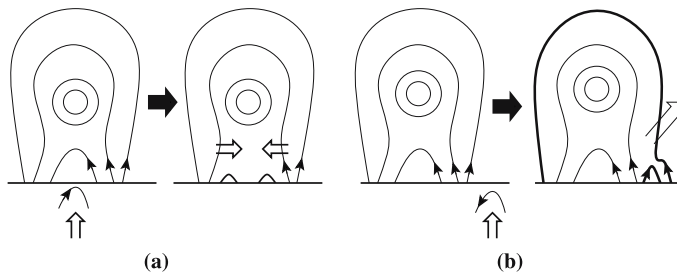


**Figure 1.** Schematic diagram of the emerging flux trigger mechanism for CMEs. **(a)** Emerging flux inside the filament channel cancels the pre-existing loops, which results in the *in situ* decrease of the magnetic pressure. Lateral magnetized plasmas are driven convergently to form a current sheet; **(b)** Emerging flux outside the filament channel reconnects with the large coronal loop, which results in the expansion of the loop. The underlying flux rope then rises and a current sheet forms near the magnetic null point.

decreases locally. Plasmas on both sides of the PIL, which are initially in equilibrium, are driven to move convergently along with the frozen-in anti-parallel magnetic field under the pressure gradient. As a result, a current sheet forms above the PIL, and the flux rope is also triggered to move slightly upward. The ensuing reconnection at the current sheet leads to the formation of a cusp-shaped two-ribbon flare and the fast eruption of the flux rope system. When the reconnection-favorable emerging flux appears outside the filament channel (say, on the right side), it reconnects with the large-scale magnetic arcades that cover the flux rope. The right leg of the arcade, which is rooted very close to the PIL, is re-connected far from the PIL on the right side of the emerging flux. The magnetic tension force along the curved field line pulls the arcades to move upward, with the flux rope following immediately. The rising flux rope pulls the overlying field lines up and a current sheet forms near the null point below the flux rope. Similarly, the magnetic reconnection at the current sheet leads to a two-ribbon flare and the fast eruption of a CME.

In this model, the onset of the CME is triggered by the localized reconnection between emerging flux and the pre-existing coronal field. Such a reconnection produces X-ray jets (and  $H\alpha$  surges if chromosphere is considered as done in Yokoyama & Shibata 1995), which correspond to the soft X-ray precursor well before the main flare as mentioned by Harrison *et al.* (1985). The numerical results also show that the impulsive phase of the main flare coincides with the acceleration phase of the CME, and after the flare peak, the CME moves with an almost constant velocity. Jing *et al.* (2004) found that about 68% of disk CMEs are associated with emerging flux. So, the onset of quite a large part of the CMEs can be explained by our model. The simulation results in this model were also found to be consistent with various observations (e.g., Zhang *et al.* 2001). In particular, Sterling & Moore (2005) analyzed a CME event, in which they found that the height profile of the filament is very similar to that in our paper. A parameter survey of this model was conducted by Xu *et al.* (2005); its image synthesis was composed by Shiota *et al.* (2005) in order to compare with Yohkoh/SXT images. Such a model was recently extended to the spherical co-ordinators (Dubey *et al.* 2006).

## 2.2 Other trigger mechanisms

Observations have shown various kinds of evolving magnetic structures, for example, converging motion of the filament channel (note that the apparent converging motion may be a result of the diffusion of magnetic polarities), shear motion, twist motion, decay of the active region, etc. Accordingly, trigger mechanisms based on these changes have also been proposed. van Ballegoijen & Martens (1989) proposed that the converging motion of magnetic arcades, by which a filament may be formed, can also lead to the destabilization of the filament; Mikić *et al.* (1988) found that after a large enough shear, the closed magnetic arcades would asymptotically approach the open field, while a resistive instability can result in the eruption. Kusano *et al.* (2004), however, found that reversed magnetic shear could also trigger the eruption. Both analytical and numerical simulations indicate that there may exist catastrophic behavior in the flux rope motions as the footpoints of the magnetic arcades converge or shear (Forbes & Priest 1995; Hu & Jiang 2001). The analytical investigation by Isenberg *et al.* (1993) illustrates that the gradual decay of the background magnetic field would also cause the flux rope to lose equilibrium catastrophically. In all of these

three cases and our emerging flux model, the essence is that the evolving magnetic structure either increases the magnetic pressure below the flux rope or decreases the magnetic tension force above the flux rope, thereby the flux rope cannot sustain its equilibrium.

Chen *et al.* (1997) and Krall *et al.* (2001) proposed that the injection of poloidal magnetic flux into the flux rope would cause the flux rope to erupt. Physically this process is similar to the kink instability model as put forward by Hood & Priest (1981) and simulated by Török and Kliem (2005). The model has been compared with observations in many cases. A modified version of the kink model, i.e., the rupture mechanism, was proposed by Sturrock *et al.* (2001) and simulated by Fan (2005), where part of the flux rope penetrates the overlying magnetic field and erupts into the IP space.

In order to circumvent the Aly's constraint, Antiochos *et al.* (1999) proposed a magnetic breakout model, i.e., only the sheared part of the closed field lines near the PIL is opened during the CME. The essence of this model is that the overlying background magnetic field reconnects with the sheared arcade at the magnetic null point above the latter, by which the constraint over the sheared arcade is removed gradually like an onion-peeling process. If such a reconnection above the arcade exists during the onset of the CME, it is expected to see soft X-ray bright loops on both sides of the sheared arcade and reverse type III radio bursts that are produced by the reconnection-accelerated electrons.

There are some other less-recognized trigger mechanisms for CMEs. Filament mass drainage, by which the filament obtains a buoyancy force, may play a role in triggering the onset of a CME (Low 2001), which was identified in one event recently (Zhou *et al.* 2006). Moreton and EIT waves, which are generated by a remote CME, often trigger a filament to oscillate, and erupt sometimes (Ballester 2006), which deserves further investigations.

### 3. Propagation of CMEs

As mentioned in section 1, there are many interesting topics related to the propagation of CMEs. Here, we just mention the EUV counterparts of propagating CMEs, i.e., EIT waves/dimmings.

#### 3.1 EIT wave/dimming observations

EIT waves were originally observed by the EIT telescope onboard the SOHO satellite as propagating wave-like fronts, with an emission enhancement ranging from 25% to less than 14%, which is followed immediately by expanding EIT dimmings (Thompson *et al.* 1998). Therefore, EIT waves and dimmings are symbiotic phenomena. One typical feature is that the bright fronts propagate only in the quiet regions, avoiding any active region. Therefore, when the large-scale magnetic configuration is simple, for instance, with only one active region on the visible disk, the EIT wave fronts are almost circular; however, when there are other active regions surrounding the source region of the eruption, the EIT waves appear in patches, managing their ways outward separately in the quiet regions.

Wills-Davey & Thompson (1999) found that EIT waves can be observed in both 195 Å (with the formation temperature  $T \sim 1.4$  MK) and 171 Å (with the formation

temperature  $T \sim 1$  MK), with more detailed structures in the  $171 \text{ \AA}$  images. Later, Zhukov & Auchere (2004) also identified EIT waves in  $284 \text{ \AA}$  (with the formation temperature  $T \sim 1.9$  MK). Since the brightenings are observed at very different temperatures, it is concluded that they are mainly due to the density enhancement, although Wills-Davey & Thompson (1999) and Chen & Fang (2005) pointed out that temperature effect is not negligible. Weak dimmings are also reported at  $304 \text{ \AA}$  (Chertok & Grechnev 2003). However, it is not sufficient to say they have imprints in the chromosphere since a coronal line Si XI  $303.32 \text{ \AA}$  and a transition region line He II  $303.78 \text{ \AA}$  are blended at the EIT  $304$  bandpass. It is generally believed that EIT waves are a phenomenon propagating in the corona. Based on the observational results in Thompson *et al.* (2000) and Harrison *et al.* (2003), Chen & Fang (2005) proposed that the ‘‘EIT waves’’ map the footprints of the CME leading edge, and the dimming region maps the bottom of the CME cavity. Therefore, EIT waves/dimmings are actually the EUV counterparts of CMEs.

### 3.2 Debates on EIT wave mechanism

Early in the 1960s, it was discovered in the  $H\alpha$  line wing that arc-shaped chromospheric perturbations propagate away from some big flares (Moreton & Ramsey 1960), which were later called Moreton waves. Such a wave, with a surprisingly large velocity of the order of  $1000 \text{ km s}^{-1}$ , was later explained by Uchida (1968) as a fast-mode wave in the corona, which sweeps the chromosphere as it propagates. Since then, it was expected to detect such a wave in the corona. It was not successful except one event observed by OSO 7 satellite (Neupert 1989). The discovery of EIT waves by SOHO/EIT, then, sparked a lot of interest, as well as controversies. It was very natural to consider the EIT waves as the ever-missing coronal counterparts of Moreton waves (or coronal Moreton waves for short), i.e., they are coronal fast-mode waves. After extrapolating the coronal magnetic field based on a potential field model, Wang (2000) and Wu *et al.* (2001) claimed that the propagating fast-mode waves in the corona can match the observed EIT wave fronts. However, it is very difficult for the fast-mode wave model to explain the typical features of EIT waves: (1) The EIT wave speeds are 3 or more times smaller than Moreton waves (Klassen *et al.* 2000); (2) Delannée & Aulanier (1999) found that EIT waves stop at the magnetic separatrix, which led them to speculate that EIT waves could be associated with magnetic rearrangement; (3) The EIT velocities are not correlated with the speeds of the type II radio bursts, the latter of which are believed to be the radio signature of the coronal fast-mode shock waves; (4) EIT wave speeds can be as low as  $50 \text{ km s}^{-1}$  (Thompson & Myers 2007), which is even below the sound speed in the corona. However, fast-mode wave speed should always be larger than the sound speed.

In order to reconcile all these discrepancies, Chen *et al.* (2002 and 2005) predict that there should exist two EUV waves associated with a CME event, i.e., the coronal Moreton wave and the EIT wave, which was later confirmed by Harra & Sterling (2003). In our model, the coronal Moreton waves correspond to the piston-driven shock over the CME rather than the blast wave from the pressure pulse in the flare, and EIT waves are generated by successive opening (or stretching) of closed field lines, which is pushed by the erupting flux rope. Each field line is pushed to expand at its top, and the deformation is transferred down to the footpoints of the field line. Whenever the leg of a field line expands, the plasma outside the field line is compressed to form

an EIT wave front, while the plasma inside is evacuated, resulting in EIT dimmings. Therefore, the model can explain both EIT waves and dimmings. The numerical results reproduce many characteristics that are obtained from observations: (1) EIT waves propagate with a velocity  $\sim 3$  times smaller than the coronal Moreton waves; (2) EIT waves stop at the magnetic separatrix between the source active region and another active region; (3) the EIT wave speed is anti-correlated with the speed of type II radio bursts.

### 3.3 Significance of EIT wave/dimming observations

- EIT waves/dimmings are the disk signatures of CMEs: Biesecker *et al.* (2002) found that whenever there is an EIT wave, there should be a CME in the coronagraph images, although the contrary is not true. As mentioned above, EIT waves/dimmings map the CME leading edge/cavity, and they are the disk signatures of the CMEs. Therefore, routine observations of EIT waves/dimmings will be an efficient way to monitor CMEs, especially those directed towards our earth.
- EIT dimmings provide an estimate of the mass supply for CMEs: CMEs are the major drivers for space weather disturbances such as geomagnetic storms. Their mass, as well as their velocity and the magnetic field, is an important factor that may influence their geomagnetic effect. Hence, the estimate of their mass in the early phase of the eruption is crucial for space weather forecast. Harrison & Lyons (2000) proposed that EIT dimmings, which are due to the plasma evacuation as in our model, can be used to estimate the CME mass.
- Large-scale coronal magnetic field can be inferred: Various efforts have been put into the measurement of the coronal magnetic field, such as the radio diagnosis, near infrared Zeeman effect measurements, and so on. Before these methods become practical, EIT waves/dimmings can provide an efficient way to diagnose the coronal magnetic field. As discussed in Chen *et al.* (2002 and 2005), EIT waves/dimmings are produced by the opening of the closed field lines covering the erupting flux rope. This means that coronal field lines should be self-closed within the dimming regions. With sufficiently high cadence of the EIT wave observations, their velocity pattern can even be used to derive the coronal magnetic field.

## 4. Prospects for the Solar Cycle 24

It is seen from the above review that our understanding of the CME initiation and propagation strongly relies on observations. For the CME initiation, it will be vital to detect the progenitor of the CME and its early evolution in order to distinguish between various trigger models. In this sense, UV coronagraph observations would be invaluable to trace the early evolution of any ongoing eruption; on the other hand, sub-surface detections of the magnetic field and motions based on the local seismology would also be helpful. For the EIT waves/dimmings, we believe that the ongoing STEREO/SECCHI observations with a high cadence would gradually uncover the veil over the spectacular phenomenon, which can then be used as a proxy for the coronal magnetic field diagnostics.

### Acknowledgements

The author thanks the referee for the comments. The research is supported by the Chinese foundations NCET-04-0445, FANEDD (200226), 2006CB806302, NSFC (10221001, 10333040, 10403003, and 106100099).

### References

- Antiochos, S. K., DeVore, C. R., Klimchuk, J. A. 1989, *Astrophys. J.*, **510**, 485.  
 Ballester, J. L. 2006, *Phil. Trans. Roy. Soc. A*, **364**, 405.  
 Biesecker, D. A., Myers, D. C., Thompson, B. J. *et al.* 2002, *Astrophys. J.*, **569**, 1009.  
 Chen, J., Howard, R. A., Brueckner, G. E. *et al.* 1997, *Astrophys. J.*, **490**, L191.  
 Chen, P. F., Fang, C. 2005, *IAU Symp.*, **226**, 55.  
 Chen, P. F., Fang, C., Shibata, K. 2005, *Astrophys. J.*, **622**, 1202.  
 Chen, P. F., Shibata, K. 2000, *Astrophys. J.*, **545**, 524.  
 Chen, P. F., Wu, S. T., Shibata, K., Fang, C. 2002, *Astrophys. J. Lett.*, **572**, L99.  
 Chertok, I. M., Grechnev, V. V. 2003, In: *Proceedings of ISCS 2003: Solar Variability as an Input to the Earths Environment*, **ESA SP-535**, 435.  
 Datlowe, D. W., Elcan, M. J., Hudson, H. S. 1974, *Solar Phys.*, **39**, 155.  
 Delannée, C., Aulanier, G. 1999, *Solar Phys.*, **190**, 107.  
 Dubey, G., Holst, B. V. D., Poedts, S. 2006, *J. Astrophys. Astron.*, **27**, 159.  
 Fan, Y. 2005, *Astrophys. J.*, **630**, 543.  
 Feynman, J., Martin, S. F. 1995, *JGR*, **100**, 3355.  
 Forbes, T. G. 2000, *J. Geophys. Res.*, **105**, 23153.  
 Forbes, T. G., Priest, E. R. 1995, *Astrophys. J.*, **446**, 377.  
 Gopalswamy, N. 2003, *Adv. Space Res.*, **31**, 869.  
 Harra, L. K., Sterling, A. C. 2003, *Astrophys. J.*, **587**, 429.  
 Harrison, R. A., Bryans, P., Simnett, S. M. *et al.* 2003, *Astron. Astrophys.*, **400**, 1071.  
 Harrison, R. A., Lyons, M. 2000, *Astron. Astrophys.*, **358**, 1097.  
 Harrison, R. A., Waggett, P. W., Bentley, R. D. *et al.* 1985, *Solar Phys.*, **97**, 387.  
 Hood, A. W., Priest, E. R. 1981, *Geophys. Astrophys. Fluid Dynamics*, **17**, 297.  
 Hu, Y. Q., Jiang, Y. W. 2001, *Solar Phys.*, **203**, 309.  
 Isenberg, P. A., Forbes, T. G., Demoulin, P. 1993, *Astrophys. J.*, **417**, 368.  
 Jing, J., Yurchyshyn, V. B., Yang, G., Xu, Y., Wang, H. 2004, *Astrophys. J.*, **614**, 1054.  
 Klassen, A., Aurass, H., Mann, G. *et al.* 2000, *Astron. Astrophys. Suppl.*, **141**, 357.  
 Krall, J., Chen, J., Duffin, R. T. *et al.* 2001, *Astrophys. J.*, **562**, 1045.  
 Kusano, K., Maeshiro, T., Yokoyama, T., Sakurai, T. 2004, *Astrophys. J.*, **610**, 537.  
 Low, B. C. 2001, *J. Geophys. Res.*, **106**, 25141.  
 Mikić, Z., Barnes, D. C., Schnack, D. D. 1988, *Astrophys. J.*, **328**, 830.  
 Moreton, G. E., Ramsey, H. E. 1960, *PASP*, **72**, 357.  
 Neupert, W. M. 1989, *Astrophys. J.*, **344**, 504.  
 Shiota, D., Isobe, H., Chen, P. F. *et al.* 2005, *Astrophys. J.*, **634**, 663.  
 Sterling, A. C., Moore, R. 2005, *Astrophys. J.*, **630**, 1148.  
 Sturrock, P. A., Weber, M., Wheatland, M. S. *et al.* 2001, *Astrophys. J.*, **548**, 492.  
 Thompson, B. J., Cliver, E. W., Nitta, N. *et al.* 2000, *GRL*, **27**, 1431.  
 Thompson, B. J., Myers, D. C. 2007, *Astrophys. J. Suppl.*, in press.  
 Thompson, B. J., Plunkett, S. P., Gurman, J. B. *et al.* 1998, *GRL*, **25**, 2465.  
 Török, T., Kliem, B. 2005, *Astrophys. J.*, **630**, L97.  
 Uchida, Y. 1968, *Solar Phys.*, **4**, 30.  
 van Ballegooijen, A. A., Martens, P. C. H. 1989, *Astrophys. J.*, **343**, 971.  
 Wang, Y.-M. 2000, *Astrophys. J.*, **543**, L89.  
 Wang, Y. M., Sheeley Jr. N. R. 1999, *Astrophys. J.*, **510**, L157.  
 Wills-Davey M. J., Thompson, B. J. 1999, *Solar Phys.*, **190**, 467.  
 Wu, S. T., Zheng, H. N., Wang, S. *et al.* 2001, *JGR*, **106**, 25089.  
 Xu, Xiao-Yan, Chen, Peng-Fei, Fang, C. 2005, *Chinese J. Astron. Astrophys.*, **5**, 636.  
 Yokoyama, T., Shibata, K. 1995, *Nature*, **375**, 42.

- Zhang, J., Dere, K. P., Howard, R. A. *et al.* 2001, *Astrophys. J.*, **559**, 452.  
Zhou, G. P., Wang, J. X., Zhang, J. *et al.* 2006, *Astrophys. J.*, **651**, 1238.  
Zhukov, A. N., Auchère, F. 2004, *Astron. Astrophys.*, **427**, 705.